ISSN 1330-3651
UDC/UDK 621.391.822:621.376.2

ANALYTICAL PERFORMANCE EVALUATION OF TIME-HOPPING PULSE POSITION AMPLITUDE MODULATION IR-UWB SYSTEMS UNDER MULTI USER INTERFERENCE

Marijan Herceg, Ratko Grbić, Tomislav Švedek

Original scientific paper

In this paper, the characteristic function (CF) method is used to derive symbol error rate (SER) expression for time-hopping impulse radio ultra–wideband (TH-IR-UWB) systems with Pulse Position Amplitude Modulation (PPAM) scheme in the presence of multi-user interference (MUI). The derived expression is validated with Monte-Carlo simulation and compared with orthogonal Pulse Position Modulation (PPM). Moreover, the analytical results are compared with Gaussian approximation (GA) of MUI which is shown to be inaccurate for medium and large signal-to-noise ratio (SNR). It is also shown that PPAM scheme outperforms PPM scheme for all SNR. At the end the influence of different system parameters on the PPAM performance is analyzed.

Key words: *characteristic function, multi-user interference, Pulse Position Amplitude Modulation, symbol error rate, ultra-wideband*

Analitička evaluacija performansi Pulsno Pozicijsko Amplitudne Modulacije u IR-UWB sustavima s vremenskim poskakivanjem u prisustvu višekorisničke smetnje

Izvorni znanstveni članak

U ovom radu je korištena metoda karakteristične funkcije (CF) za izvod učestalosti pogreške simbola (SER) u impulsnim ultra-širokopojasnim radio sustavima s vremenskim poskakivanjem (TH-IR-UWB) i Pulsno Pozicijsko Amplitudnom Modulacijom (PPAM) u prisustvu više-korisničke smetnje (MUI). Dobiveni izraz je potvrđen Monte-Karlo simulacijom i uspoređen s ortogonalnom Pulsno Pozicijskom Modulacijom (PPM). Nadalje, analitički rezultati su uspoređeni s Gaussovom aproksimacijom (GA) više-korisničke smetnje, za koju je pokazano da je neprecizna za srednje i velike odnose signal-šum (SNR). Još je pokazano da PPAM nadmašuje PPM za sve odnose SNR. Na kraju je analiziran utjecaj različitih parametara modulacije na svojstva PPAM.

Ključne riječi: *karakteristična funkcija, Pulsno Pozicijsko Amplitudna Modulacija, učestalost pogreške simbola, ultra-široki pojas, više-korisnička smetnja*

1 Introduction
Uvod

Trends in modern communication systems place high demands on low power consumption, high speed transmission and anti-interference characteristics. Therefore impulse radio ultra–wideband (IR-UWB) [1] radio systems have recently gained increased popularity. Since IR-UWB symbols are transmitted with short pulses (< 2 ns), in IR-UWB systems, energy has been spread over the frequency bands of up to 10 GHz. UWB pulses have to follow strict regulations concerning power and spectrum restrictions defined by local authorities, like the Federal Communications Commission (FCC) [2] in the USA. Because of power and spectral properties of transmitted UWB pulses, different type of orthogonal pulse shapes are being used to provide higher spectral efficiency [3], [4]. Derivation of Gaussian pulse and modified Hermite pulses (MHP), usually called Hermites [5], provide wide range of variety pulse combinations for IR-UWB transmission and for that reason these are the most common pulse shapes. The state-of-the art in IR-UWB systems presents many applicable modulation methods like Pulse Amplitude Modulation (PAM), PPM, Pulse Shape Modulation (PSM), on-off-keying (OOK), binary phase-shift keying (BPSK) and Pulse Interval Modulation (PIM) [6]. A combination of these modulation techniques (hybrid techniques) can provide system improvements in terms of the error probability, a higher data rate, a less complex receiver or less power consumption. Many hybrid techniques for IR-UWB communication systems have been applied recently, such as Biorthogonal Pulse Position Modulation (BPPM) [7], OOK-PSM [8], PPM-PSM [9], hybrid Shape-Amplitude Modulation [10], and Multi Pulse Position-Amplitude Modulation [11]. Since the first time that multiple-access time hopping (TH) UWB systems was presented [1] lots of researches have been done in order to analyze multi-user interference (MUI) performance over additive white Gaussian noise (AWGN). The most common method used for representing MUI is Gaussian approximation (GA) [12], while authors in [13], [14] show that GA method is not accurate for medium and large signal-to-noise ratio.

The characteristic function (CF) method for calculating bit error rate (BER) was presented in [15], while the analytical method of calculating BER for TH-PPM and TH-BPSK UWB systems based on CF is given in [16], [17] and later extended on N - orthogonal PPM in [18]. Exact comparison of TH-IR-UWB and direct sequence (DS) IR-UWB systems performance is given in [19].

In this paper we extend the CF analysis on Pulse Position Amplitude Modulation (PPAM) scheme which is first presented in [20]. PPAM combines N-ary PPM and M-ary PAM to construct MN-ary PPAM signal. It is shown that PPAM has better performance and lower complexity than orthogonal PPM for the same throughput. It is also shown that GA significantly underestimates error rate performance for medium and large SNR.

This paper is organized as follows: Section 2 describes the TH-IR-UWB PPAM system model. In Section 3 the accurate analytical expression for PPAM error probability is derived. The numerical results are given in Section 4 while some conclusions are given in Section 5.

2 TH-IR-UWB system model
Model TH-IR-UWB sustava

The asynchronous PPAM TH-IR-UWB system is in detail described in [20]. Typical MN – ary PPAM signal for k-th users can be written as

$$s^{(k)} = \sum_{l=-\infty}^{\infty} \sum_{j=lN_s}^{(l+1)N_s-1} A_{b_l^{(k)}} \sqrt{\frac{E_s}{N_s}}\, p\left(t - jT_f - c_j^{(k)}T_c - d_l^{(k)}\delta\right), \quad (1)$$

where

$$A_{b_l^{(k)}} \sqrt{E_s / N_s}$$

is one of the M possible amplitude levels with

$$A_{b_l^{(k)}} = 2b_l^{(k)} - 1 - M,\ \ 1 \le b_l^{(k)} \le M,\ E_s = 3E_{av}/(M^2-1)$$

is energy per symbol, and E_{av} is average energy per symbol. N_s is number of pulses used to transmit a single symbol, l is the symbol index, $p(t)$ is the signal pulse with duration T_p and normalized energy

$$\int_{-\infty}^{\infty} p^2(t)\mathrm{d}t = 1.$$

T_f is frame duration which determinates symbol duration as $T_s = N_s T_f$. $c_j^{(k)}$ is pulse shift pattern also called TH sequence of the k-th user which is pseudorandom and each element assumes any value from $0 \le c_j^{(k)} \le N_h - 1$. N_h is the number of hops and T_c is the chip duration which should satisfy the condition $N_h T_c < T_f$. δ is time shift parameter and it is set to be $>T_p$ which provides orthogonality between pulse positions within symbol. $d_l^{(k)} \in \{0,\dots,N-1\}, b_l^{(k)} \in \{1,\dots,M\}$ are determined with l-th data symbol of the k-th source and represents the position and amplitude level of pulse in MN-ary PPAM symbol

In our work we have without loss of generality assumed that [17]:

- User 1 is a desired user and other $N_u - 1$ users are interference.
- TH code for first user is $c_j^{(1)} = 0, \forall j$.
- $d_0^{(1)}$ and $b_0^{(1)}$ are transmitted.
- Perfect code synchronization at the receiver.

If AWGN channel model is used, the signal received in the multi-user environment is given as

$$r(t) = \sum_{k=1}^{N_u} A_k s^{(k)}(t - \tau_k) + n(t), \quad (2)$$

where N_u is number of users, τ_k is time delay of the k-th user, A_k is channel attenuation for the k-th user and $n(t)$ is additive white Gaussian noise with two sided power spectral density $N_0/2$.

In order to demodulate received signal it is assumed that the correlator based receiver shown in Fig. 1 is used.

As it can be seen from Fig. 1 PPAM receiver in the i-th branch correlates received signal with template waveform which is for the first user given as

$$\psi_i^{(1)}(t) = \sum_{j=0}^{N_s} \sqrt{\frac{N_s}{E_s}}\, p\left[t - jT_f - c_j^{(1)}T_c - (i-1)\delta - \tau_1\right], \quad i = 1,\dots N. \quad (3)$$

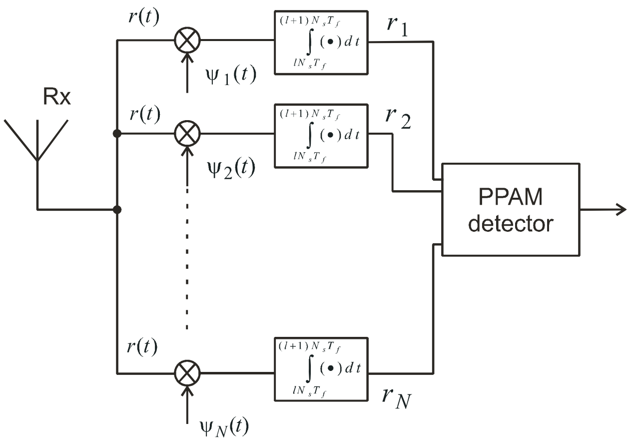

Figure 1 *PPAM receiver*
Slika 1. *PPAM prijemnik*

In our work we have assumed that the pulse shape used for data transmission (also the template pulse) is the second derivation of Gaussian pulse given by [17]

$$p(t) = \left[1 - 4\pi\left(\frac{t}{\tau_p}\right)^2\right]\exp - \left[2\pi\left(\frac{t}{\tau_p}\right)^2\right], \quad (4)$$

where τ_p is time normalization factor. Defining autocorrelation function of $p(t)$ as

$$R(x) = \int_{-\infty}^{\infty} p(t)p(t-x)\mathrm{d}t, \quad (5)$$

we can then write $R(x)$ as

$$R(x) = \left[1 - 4\pi\left(\frac{x}{\tau_p}\right)^2 + \frac{4\pi^2}{3}\left(\frac{x}{\tau_p}\right)^4\right]\exp\left[-\pi\left(\frac{x}{\tau_p}\right)^2\right]. \quad (6)$$

3 Analytical derivation of symbol error rate
Analitički izvod učestalosti pogreške simbola

In order to derive symbol error rate (SER) expression of the PPAM TH-IR-UWB system we have assumed that the first user is the desired one and that the 0-th transmitted information symbol is sent and that it is equal to $d_0^{(1)} = 0$, $b_0^{(1)} = m$. We will further assume that $c_j^{(1)} = 0$, for all j. Using the receiver shown in Fig. 1 we can define the correlators' output with vector $\boldsymbol{r} = [r_1 r_2 \dots r_N]$, where r_i is

$$r_i = \sum_{j=0}^{N_s-1} \int_{jT_f}^{(j+1)T_f} r(t)\psi_i^{(1)}(t)\mathrm{d}t = \begin{cases} S + I_i + N_i, & i = 1 \\ I_i + N_i, & i = 2,\dots,N. \end{cases} \quad (7)$$

$S = A_m N_s R(0)$ is contribution of desired transmitted information symbol $d_0^{(1)}, b_0^{(1)}$ to decision statistic r_1. N_i is AWGN component at the output of the i-th correlator modelled as Gaussian random variable with zero mean and variance $\sigma_n^2 = N_s^2 R(0)/2(E_s/N_0)$. I_i is MUI component at the output of the i-th correlator and it is given as

$$I_i = \sum_{k=2}^{N_u} \int_0^{N_s T_f} s^{(k)}(t - \tau_k)\psi_i^{(1)}(t)\mathrm{d}t. \quad (8)$$

From [20, 21] it can be seen that PPAM detector decides which symbol is sent in favour of r_i with the largest magnitude, and then the sign and the value of that magnitude is used to decide which of the M possible amplitudes, i.e. m is sent. Then the probability of correct decision if $d_0^{(1)} = 0, b_0^{(1)} = m$ is sent, can be given as

$$P_{\mathrm{C\_PPAM}} = \frac{1}{M}\left(\begin{array}{l} \sum_{m=2}^{M-1} \int_{(A_m-1)\sqrt{E_s}}^{(A_m+1)\sqrt{E_s}} P(\bigcap_{i=2}^{N} |r_i| < r_{m1} | d_0^{(1)} = 0) p(r_{m1}) \mathrm{d}r_{m1} \\ + \left. \int_{-\infty}^{(A_m+1)\sqrt{E_s}} P(\bigcap_{i=2}^{N} |r_i| < r_{m1} | d_0^{(1)} = 0) p(r_{m1}) \mathrm{d}r_{m1} \right|_{m=1} \\ + \left. \int_{(A_m-1)\sqrt{E_s}}^{\infty} P(\bigcap_{i=2}^{N} |r_i| < r_{m1} | d_0^{(1)} = 0) p(r_{m1}) \mathrm{d}r_{m1} \right|_{m=M} \end{array} \right), \quad (9)$$

where r_{m1} is output of the first correlator when the m-th amplitude level is sent, while $p(r_{m1})$ is its probability density function (PDF). Finally, the probability of a symbol error for PPAM is

$$P_{\mathrm{e\_PPAM}} = 1 - P_{\mathrm{c\_PPAM}} \,. \quad (10)$$

Following the same procedure as in [21] we will first derive probability that

$$P(\bigcap_{i=2}^{N} | I_i + N_i | < r_{m1}) = P(\bigcap_{i=2}^{N} - r_{m1} < I_i + N_i < r_{m1}). \quad (11)$$

To derive the probability that $P(-r_{m1} < I_i + N_i < r_{m1})$ using CF method we will write I_i as

$$\begin{aligned} I_i = & \sum_{k=2}^{N_u} \sum_{j=0}^{N_s-1} \sum_{j'=-\infty}^{\infty} \int_{-\infty}^{\infty} A_{b^{(k)}_{\lfloor j'/N_s \rfloor}} \cdot \\ & \cdot p(t - j'T_f - c_{j'}^{(k)} T_c - d^{(k)}_{\lfloor j'/N_s \rfloor} \delta - \tau_k) \cdot \\ & \cdot p(t - jT_f - (i-1)\delta - \tau_1) \mathrm{d}t = \\ = & \sum_{k=2}^{N_u} \sum_{j=0}^{N_s-1} \sum_{j'=-\infty}^{\infty} A_{b^{(k)}_{\lfloor j'/N_s \rfloor}} \cdot \\ & \cdot R((j'-j)T_f + c_{j'}^{(k)} T_c + (d^{(k)}_{\lfloor j'/N_s \rfloor} - (i-1))\delta + (\tau_k - \tau_1)). \end{aligned} \quad (12)$$

Due to the property that $R(x)$ is nonzero only for $|x| < T_p$ and assuming that [12]

$$N_h T_c < T_f / 2 - 2T_p, \quad (13)$$

which implies that only one pulse from each interfering user in each frame contributes to the MUI which implies that $j' = j$. The difference between time arrivals of user one and user k can be modelled as [12]

$$\tau_k - \tau_1 = j_k T_f + \alpha_k, \quad -\frac{T_f}{2} \le \alpha_k < \frac{T_f}{2}, \quad (14)$$

where $j_k T_f$ is time difference between $\tau_k - \tau_1$ while j_k is rounded to the nearest integer and α_k is the error in the rounding process which is modelled as random variable uniformly distributed over interval $[-T_f/2, T_f/2]$. Then (12) can be rewritten as

$$I_i = \sum_{k=2}^{N_u} \sum_{j=0}^{N_s-1} A_{b^{(k)}_{\lfloor (j+j_k)/N_s \rfloor}} R_i(d^{(k)}_{\lfloor (j+j_k)/N_s \rfloor} \delta + c_j^{(k)} T_c + \alpha_k), \quad (15)$$

where

$$R_i(x) = R(x - (i-1)\delta). \quad (16)$$

The interfering signal $d^{(k)}_{\lfloor (j+j_k)/N_s \rfloor}, b^{(k)}_{\lfloor (j+j_k)/N_s \rfloor}$ may change value during transmission of symbol 0 so we can rewrite (15) as

$$I_i = \sum_{k=2}^{N_u} I_i^{(k)}, \quad (17)$$

where

$$I_i^{(k)} = \left(\sum_{j=0}^{\gamma_k - 1} A_{b_0^{(k)}} R_i(\Delta t_{0,j}^{(k)}) + \sum_{j=\gamma_k}^{N_s-1} A_{b_1^{(k)}} R_i(\Delta t_{1,j}^{(k)}) \right), \quad (18)$$

with

$$\begin{aligned} \Delta t_{0,j}^{(k)} &= d_0^{(k)} \delta + c_j^{(k)} T_c + \alpha_k, \\ \Delta t_{1,j}^{(k)} &= d_1^{(k)} \delta + c_j^{(k)} T_c + \alpha_k. \end{aligned} \quad (19)$$

Subscript 0 and 1 represent two neighbor symbols of the k-th user that overlap with transmission time of the first user symbol 0, γ_k is random variable uniformly distributed over $[0, N_s - 1]$. If we write

$$I_i^{(k)} = X_i^{(k)} + Y_i^{(k)}, \quad (20)$$

where

$$X_i^{(k)} = \sum_{j=0}^{\gamma_k - 1} A_{b_0^{(k)}} R_i(t_{0,j}^{(k)}), \quad (21)$$

$$Y_i^{(k)} = \sum_{j=\gamma_k}^{N_s-1} A_{b_1^{(k)}} R_i(t_{1,j}^{(k)}), \quad (22)$$

then CF of $X_i^{(k)}$ conditioned on $d_0^{(k)}, b_0^{(k)}$, α_k and γ_k is

$$\begin{aligned} & \phi_{X_i^{(k)}|d,b,\alpha,\gamma}(\omega) = \\ & E\left[\exp(j\omega \sum_{j=0}^{\gamma_k - 1} A_{b_0^{(k)}} R_i(\Delta t_{0,j}^{(k)})) \,|\, d_0^{(k)} = d, b_0^{(k)} = b, \alpha_k = \alpha, \gamma_k = \gamma) \right] = \\ & \left(\frac{1}{N_h} \sum_{h=0}^{N_h - 1} \exp(j\omega A_b R_i(d\delta + hT_c + \alpha)) \right)^{\gamma}, \end{aligned} \quad (23)$$

where $E[*]$ is mean value operator. The upper expression comes from the fact that $c_j^{(k)}$ can have any value in $\{0, 1, ..., N_h - 1\}$ with equal probability. Assuming that all symbols are equally likely and using the theorem of total probability we can write

$$\phi_{X_i^{(k)}|\alpha,\gamma}(\omega)=\frac{1}{MNN_h^{\gamma}}\sum_{m=0}^{N-1}\sum_{i=1}^{M}\left(\sum_{h=0}^{N_h-1}\exp(jA_m\omega R_i(m\delta+hT_c+\alpha))\right)^{\gamma}. \quad (24)$$

Using the same procedure the CF of $Y_i^{(k)}$ is

$$\phi_{Y_i^{(k)}|\alpha,\gamma}(\omega)=\frac{1}{NN_h^{N_s-\gamma}}\sum_{m=0}^{N-1}\sum_{i=1}^{M}\left(\sum_{h=0}^{N_h-1}\exp(jA_m\omega R_i(m\delta+hT_c+\alpha))\right)^{N_s-\gamma}. \quad (25)$$

Assuming that data sequence of the k-th user and each user chip sequence is independent we may write the CF of $I_i^{(k)}$ as

$$\phi_{I_i^{(k)}|\alpha,\gamma}(\omega)=\phi_{X_i^{(k)}|\alpha,\gamma}(\omega)\phi_{Y_i^{(k)}|\alpha,\gamma}(\omega). \quad (26)$$

After further averaging of $\phi_{I_i^{(k)}|\alpha,\gamma}(\omega)$ over α and γ we may write

$$\phi_{I_i^{(k)}}(\omega)=\frac{1}{N_sT_f}\int_{-T_f/2}^{T_f/2}\sum_{n=0}^{N_s-1}\phi_{I_i^{(k)}|\alpha,n}(\omega)\mathrm{d}\alpha . \quad (26)$$

At the end the total MUI of (N_u–1) independent users can be written as

$$\phi_{I_i}(\omega)=\prod_{k=2}^{N_u}\phi_{I_i^{(k)}}(\omega) . \quad (28)$$

The CF of the N_i is

$$\phi_{N_i}(\omega)=\exp(-\omega^2\sigma_n^2/2) . \quad (29)$$

Using the independence of MUI and AWGN we can write the conditional probability by applying the relationship between the CF and cumulative density function (CDF) of random variable as [17]

$$F_i(\lambda)=\frac{1}{2}+\frac{1}{\pi}\int_0^{\infty}\frac{\sin(\lambda\omega)}{\omega}\phi_{\Lambda_i}(\omega)\mathrm{d}\omega, \quad (30)$$

where

$$\phi_{\Lambda_i}(\omega)=\phi_{I_i}(\omega)\phi_{N_i}(\omega) . \quad (31)$$

At the end we can write

$$P(\bigcap_{i=2}^{N}-r_{m1}<I_i+N_i<r_{m1})=\prod_{i=2}^{N}(F_i(r_{m1})-F_i(-r_{m1})) . \quad (32)$$

From (9), it can be seen that in order to obtain accurate error performance of PPAM the PDF of r_{m1} has to be derived. The r_1 is defined as $r_{m1}=A_mN_sR(0)+I_1+N_1$, where I_1 is modelled as random variable with CF given as (27), while $A_mN_sR(0)+N_1$ can be modelled as Gaussian random variable with mean $A_mN_sR(0)$ and variance σ_n^2, and its CF is given as

$$\phi_{N_1}(\omega)=\exp(iA_mN_sR(0)\omega-\omega^2\sigma_n^2/2) . \quad (33)$$

Using the inverse Fourier transform the PDF of r_{m1} can be obtained as

$$p(r_{m1})=\frac{1}{2\pi}\int_{-\infty}^{\infty}\phi_{N_1}(\omega)\phi_{I_1}(\omega)\exp(-i\omega r_{m1})\mathrm{d}r_{m1}. \quad (34)$$

4
Numerical results
Numerički rezultati

All numerical results in this paper are obtained using Matlab, while the Monte Carlo simulation is used to validate results.

In Fig. 2 analytically obtained SER values for PPAM with $M = N = 2$ and $N_s = 2, 4, 8$ are compared with results obtained by the Monte Carlo simulation as well as by Gaussian approximation for MUI. It can be seen that GA approximate well SER for lower signal-to-noise ratio (SNR), while for higher (>6 dB) the SNR values disagreement is very high. It is the result of the fact that for smaller SNR values AWGN is dominant, while for larger SNR values MUI is dominant and then MUI cannot be well approximated with GA. Also as expected with increase of N_s SER performance increases significantly.

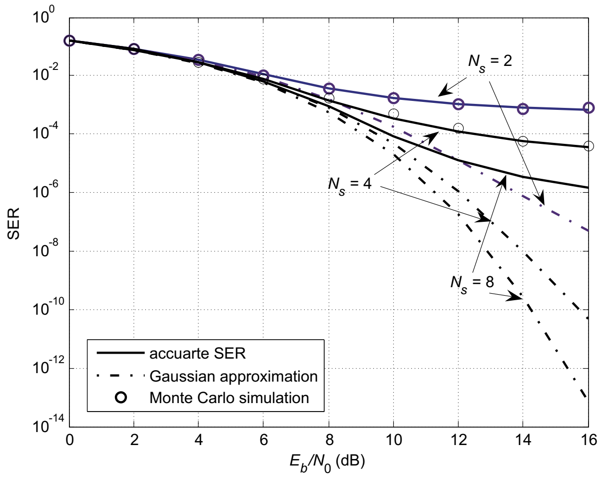

Figure 2 *Accurate analytical SER of PPAM versus E_b/N_0 with system parameters $N = M = 2$, $N_s = 2, 4, 8$, $T_f = 50$ ns, $T_c = N \cdot 0{,}9$ ns, $N_h = 8$, $\tau_p=0{,}2877$ ns, $\delta = 0{,}72$ ns, $N_u = 8$*

Slika 2. *Točni analitički SER od PPAM-a u odnosu na E_b/N_0* s parametrima *$N = M = 2$, $N_s = 2, 4, 8$, $T_f = 50$ ns, $T_c = N \cdot 0{,}9$ ns, $N_h = 8$, $\tau_p=0{,}2877$ ns, $\delta = 0{,}72$ ns, $N_u = 8$*

In Fig. 3 PPAM with different modulation levels M and N for the same bit rate which is set to 15 Mb/s is compared. It can be seen that PPAM with $M = 2$ and $N = 8$ has the best SER performance for smaller SNR values, while PPAM with $M = N = 2$ and $M = 2$, $N = 4$ has better SER performance for higher SNR values. It comes from the fact that in order to satisfy condition (13) for the fixed bit rate, due to the longer chip time, PPAM with higher modulation level has smaller N_h value, which is an important parameter for decreasing MUI.

Fig. 4 shows dependence of the SER performance on number of users N_u for different modulation levels and bit rate 15 Mb/s. The PPAM with $M = 2$ and $N = 8$ has the worst performance due to the fact that N_h is smaller.

Finally we compared orthogonal PPM and PPAM with $M = 2$, $N = 4$ for fixed bit rate in Fig. 5. It can be seen that PPAM outperforms PPM for all SNR values. For example for SNR = 16 dB and $N_s = 2$ SER of PPAM is 4×10^{-4} while SER of PPM is $1{,}2\times10^{-3}$. For $N_s = 4$ SER is $1{,}4\times10^{-4}$ for PPAM and 6×10^{-4} for PPM.

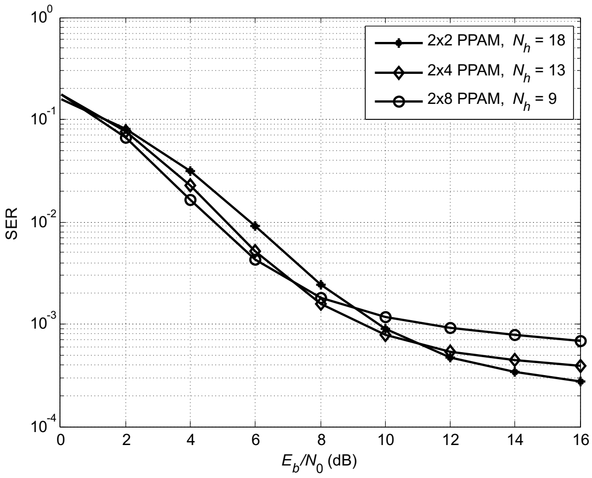

Figure 3 Comparison of PPAM with different modulation level versus E_b/N_0 for fixed bit rate (15 Mb/s). System parameters are $N_s = 2$, $T_c = N \cdot 0{,}9$ ns, $\tau_p = 0{,}2877$ ns, $\delta = 0{,}72$ ns, $N_u = 8$

Slika 3. *Usporedba PPAM-a s različitim nivoima modulacije u odnosu na E_b/N_0 za fiksnu brzinu prijenosa (15 Mb/s). Parametri sustava su $N_s = 2$, $T_c = N \cdot 0{,}9$ ns, $\tau_p = 0{,}2877$ ns, $\delta = 0{,}72$ ns, $N_u = 8$*

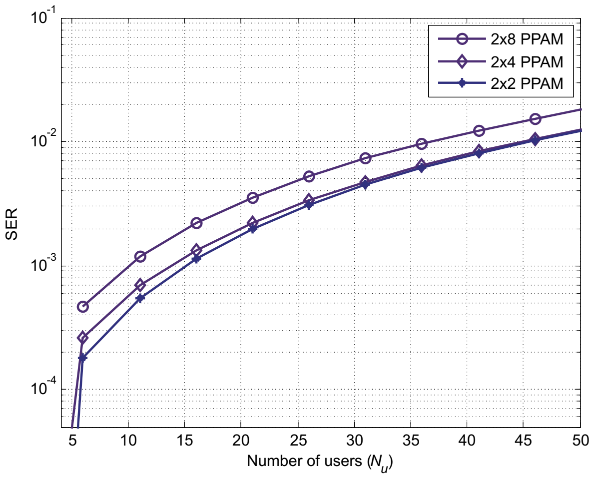

Figure 4 Comparison of PPAM with different modulation level versus N_u for fixed bit rate (15 Mb/s). System parameters are $N_s = 2$, $T_c = N \cdot 0{,}9$ ns, $\tau_p = 0{,}2877$ ns, $\delta = 0{,}72$ ns, SNR = 15 dB

Slika 4. *Usporedba PPAM-a s različitim nivoima modulacije u odnosu na N_u za fiksnu brzinu prijenosa (15Mb/s). Parametri sustava su $N_s = 2$, $T_c = N \cdot 0{,}9$ ns, $\tau_p = 0{,}2877$ ns, $\delta = 0{,}72$ ns, SNR = 15 dB*

5 Conclusion
Zaključak

In this paper, the accurate analytical expression for average SER is derived for PPAM TH-IR-UWB systems under MUI and compared with GA and the Monte Carlo simulation. It is shown that GA is accurate for small SNR values, while for larger values there is large aberration between GA and CF method. The PPAM scheme is also compared with PPM scheme where it can be seen that PPAM has better performance than PPM with half hardware complexity (fewer correlators). Due to this property PPAM scheme is attractive for TH-IR-UWB communication systems.

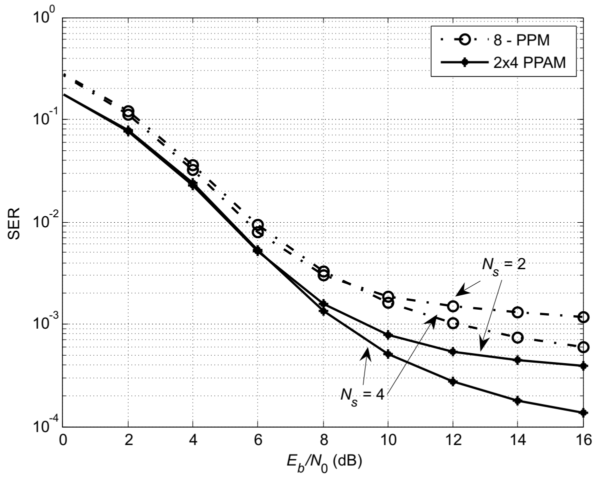

Figure 5 Comparison of PPAM and orthogonal PPM with different modulation level versus E_b/N_0 for fixed bit rate (15 Mb/s). System parameters are, $T_c = N \cdot 0{,}9$ ns, $\tau_p = 0{,}2877$ ns, $\delta = 0{,}72$ ns, $N_u = 8$, for $N_s=2$, $N_h = 13$ (6 for PPM) and for $N_s = 4$, $N_h = 6$ (3 for PPM)

Slika 5. *Usporedba PPAM-a s ortogonalnim PPM-om za različite nivoe modulacije u odnosu na E_b/N_0 za fiksnu brzinu prijenosa (15 Mb/s). Parametri sustava su $T_c = N \cdot 0{,}9$ ns, $\tau_p = 0{,}2877$ ns, $\delta = 0{,}72$ ns, $N_u = 8$, za $N_s=2$, $N_h = 13$ (6 za PPM) and for $N_s = 4$, $N_h = 6$ (3 za PPM)*

6 References
Literatura

[1] Scholtz, R. A. Multiple access with time-hopping impulse modulation. // *Proc. IEEE Military Commun. Conf.*, October 1993, pp. 11-14.

[2] FCC, Revision of part 15 of the commission's rules regarding ultra-wideband transsmision systems. // *Federal Communications Commission*, ET Docket (2002), pp. 98–153.

[3] Kim, Y.; Jang, B.; Shin, C.; Womack, B. F. Orthonormal pulses for high data rate communications in indoor UWB systems. // *IEEE Communications Letter*, 9, 5(2005), pp. 405–407.

[4] Da Silva, J. A. N.; De Campos, M. L. R. Method for Obtaining Spectrally Efficient Orthogonal UWB Pulse Shapes. // *Internacional Telecommunications Symposium*, Fortaleza-CE, Brazil, Septemper 3–6, 2006.

[5] Ghavami, M.; Michael, L. B.; Kohno, R. Ultra Wideband Signals and Systems in Communication Engineering. John Wiley & Sons, Ltd, 2004.

[6] Herceg, M.; Švedek, T.; Matić, T. Pulse Interval Modulation for Ultra-High Speed IR-UWB Communications Systems. // EURASIP Journal on Advances in Signal Processing, 2010.

[7] Zhang, H.; Gulliver,; T. A. Biorthogonal Pulse Position Modulation for Time-Hopping Multiple-Access UWB Communications. // IEEE Trans. On Wireless Comm., 4, 3(2005), pp. 1154–1162.

[8] Majhi, S.; Madhukumar, A. S. Combining OOK with PSM Modulation for TH-UWB Radio Systems: A Performance Analysis. // *EURASIP Journal on Wireless Comm. and Networking*, 2008.

[9] Mitchell, C. J.; Abreu, G.; Kohno, R. Combined Pulse Shape and Pulse Position Modulation for High Data Rate Transmissions in Ultra-Wideband Communications. // International Journal of Wireless Information Networks, 10, 4(2003), pp. 167–178.

[10] Herceg, M.; Matic, T.; Svedek, T. Performances of hybrid Amplitude Shape Modulation for UWB communications systems over AWGN channel in the single and multi-user environment. // Radioengineering Journal, 18, 3(2009).

[11] Herceg, H.; Zagar, D.; Galic, D. Multi Pulse Position Amplitude Modulation for ultra-high speed Time-Hopping UWB communication systems over AWGN channel. // 4rd International Symposium on Communications, Control and Signal Processing (ISCCSP 2010), 113, March 2010.
[12] Win, M. Z.; Scholtz, R. A. Ultra-wide bandwidth time-hopping spread-spectrum impulse radio for wireless multiple-access communications. // IEEE Trans. Commun., 48, 4(2000), pp. 679–689.
[13] Durisi, G.; Romano, G. On the validity of Gaussian approximation to characterize the multiuser capacity of UWB TH PPM, // in Proc. IEEE Conf. Ultra Wide-band Systems and Technologies, Baltimore, USA, May 2002, pp. 157–161.
[14] Durisi, G.; Benedetto, S. Performance evaluation of TH-PPM UWB systems in the presence of multiuser interference. // IEEE Commun. Lett., 7, 5(2003), pp. 224–226.
[15] Cheng, J.; Beaulieu, N. C. Accurate DS-CDMA bit error probabilty calculation in Rayleigh fading. // IEEE Trans. Wireless Commun., 1, 1(2002), pp. 3–15.
[16] Hu, B.; Beaulieu, N. C. Exact bit error rate analysis of TH-PPM UWB systems in presence of multiple access interference. // IEEE Commun. Lett., 7, 12(2003), pp. 572–574.
[17] Bo, H.; Beaulieu, N. C. Accurate evaluation of multiple-access performance in TH-PPM and TH-BPSK UWB systems. // IEEE Trans. Commun., 52, 10(2004), pp. 1758–1766.
[18] Zhou, Q. F.; Lau, F. C. M. Analytical Performance of *M*-ary Time-Hopping Orthogonal PPM UWB Systems under Multiple Acces Interference. // IEEE Trans. Commun., 56, 11(2008), pp. 1780–1784.
[19] Bo, H.; Beaulieu, N.C. Accurate performance evaluation of time-hopping and direct-sequence UWB systems in multi-user interference. // IEEE Trans. Commun., 53, 6(2005), pp. 1053–1062.
[20] Zhang, H.; Li, W.; Gulliver, T. A. Pulse Position Amplitude Modulation for Time-Hopping Multiple-Access UWB Communications, // IEEE Trans. on Comm., 53, 8(2005), pp. 895–900.
[21] J. G. Proakis, Digital Communications, 4th ed. McGraw-Hill, New York, 2001.

Authors' addresses
Adrese autora

Dr. sc. Marijan Herceg
Faculty of Electrical Engineering
J. J. Strossmayer University of Osijek
Kneza Trpimira 2B
HR-31000 Osijek, Croatia
email: marijan.herceg@etfos.hr

Ratko Grbić, dipl.ing.
Faculty of Electrical Engineering
J. J. Strossmayer University of Osijek
Kneza Trpimira 2B
HR-31000 Osijek, Croatia
email: ratko.grbic@etfos.hr

Prof. dr. sc. Tomislav Švedek
Faculty of Electrical Engineering
J. J. Strossmayer University of Osijek
Kneza Trpimira 2B
HR-31000 Osijek, Croatia
email: tomislav.svedek@etfos.hr